

Resolving ice cloud optical thickness biases between CALIOP and MODIS

R. E. Holz et al.

This discussion paper is/has been under review for the journal Atmospheric Chemistry and Physics (ACP). Please refer to the corresponding final paper in ACP if available.

Resolving ice cloud optical thickness biases between CALIOP and MODIS using infrared retrievals

R. E. Holz¹, S. Platnick², K. Meyer³, M. Vaughan⁴, A. Heidinger⁵, P. Yang⁶, G. Wind⁷, S. Dutcher¹, S. Ackerman¹, N. Amarasinghe⁷, F. Nagle¹, and C. Wang⁸

¹University of Wisconsin-Madison Space Science and Engineering Center, Madison, WI, USA

²NASA Goddard, Goddard, MD, USA

³GESTAR/USRA, Columbia, MD, USA

⁴NASA Langley, Langley, VA, USA

⁵NOAA, Madison, WI, USA

⁶Texas A and M University, College Station, TX, USA

⁷SSAI, College Park, MD, USA

⁸University of Maryland, Maryland, MD, USA

Received: 1 September 2015 – Accepted: 16 September 2015 – Published: 29 October 2015

Correspondence to: R. E. Holz (reholz@ssec.wisc.edu)

Published by Copernicus Publications on behalf of the European Geosciences Union.

Title Page

Abstract

Introduction

Conclusions

References

Tables

Figures



Back

Close

Full Screen / Esc

Printer-friendly Version

Interactive Discussion



Abstract

Despite its importance as one of the key radiative properties that determines the impact of upper tropospheric clouds on the radiation balance, ice cloud optical thickness (IOT) has proven to be one of the more challenging properties to retrieve from space-based remote sensing measurements. In particular, optically thin upper tropospheric ice clouds (cirrus) have been especially challenging due to their tenuous nature, extensive spatial scales, and complex particle shapes and light scattering characteristics. The lack of independent validation motivates the investigation presented in this paper, wherein systematic biases between MODIS Collection 5 (C5) and CALIOP Version 3 (V3) unconstrained retrievals of tenuous IOT (< 3) are examined using a month of collocated A-Train observations. An initial comparison revealed a factor of two bias between the MODIS and CALIOP IOT retrievals. This bias is investigated using an infrared (IR) radiative closure approach that compares both products with MODIS IR cirrus retrievals developed for this assessment. The analysis finds that both the MODIS C5 and the unconstrained CALIOP V3 retrievals are biased (high and low, respectively) relative to the IR IOT retrievals. Based on this finding, the MODIS and CALIOP algorithms are investigated with the goal of explaining and minimizing the biases relative to the IR. For MODIS we find that the assumed ice single scattering properties used for the C5 retrievals are not consistent with the mean IR COT distribution. The C5 ice scattering database results in the asymmetry parameter (g) varying as a function of effective radius with mean values that are too large. The MODIS retrievals have been brought into agreement with the IR by adopting a new ice scattering model for Collection 6 (C6) consisting of a modified gamma distribution comprised of a single habit (severely roughened aggregated columns); the C6 ice cloud optical property models have a constant $g \approx 0.75$ in the mid-visible spectrum, 5–15% smaller than C5. For CALIOP, the assumed lidar ratio for unconstrained retrievals is fixed at 25 sr for the V3 data products. This value is found to be inconsistent with the constrained (predominantly nighttime) CALIOP retrievals. An experimental data set was produced using a modified lidar ra-

Resolving ice cloud optical thickness biases between CALIOP and MODIS

R. E. Holz et al.

Title Page

Abstract

Introduction

Conclusions

References

Tables

Figures



Back

Close

Full Screen / Esc

Printer-friendly Version

Interactive Discussion



5 tio of 32 sr for the unconstrained retrievals (an increase of 28 %), selected to provide consistency with the constrained V3 results. These modifications greatly improve the agreement with the IR and provide consistency between the MODIS and CALIOP products. Based on these results the recently released MODIS C6 optical products use the single habit distribution given above, while the upcoming CALIOP V4 unconstrained algorithm will use higher lidar ratios for unconstrained retrievals.

1 Introduction

10 While clouds represent one of the largest modulators of Earth's radiation, with their impact dependent on a variety of cloud physical and radiative properties, they remain one of the more difficult components to represent in global climate models (Jiang et al., 2012). Passive satellite observational datasets such as those from MODIS (Moderate Resolution Imaging Spectroradiometer), AVHRR (Advanced Very High Resolution Radiometer), HIRS (High-spectral Infrared Sounder), and ISCCP (International Satellite Cloud Climatology Project) provide long-term, global cloud observations (Heidinger et al., 2013; King et al., 2013, 2003; Rossow, 1991; Rossow and Schiffer, 15 1999; Wylie and Menzel, 1999). However assessing the uncertainties in the cloud radiative properties retrieved by these sensors has proved to be a complex and difficult task. Until recently, validation of these retrievals was limited to ground and aircraft inter-comparisons. But with the successful launch of CALIPSO (Cloud-Aerosol Lidar and Infrared Pathfinder Satellite Observations) and CloudSat in April 2006 as part of the NASA-led Afternoon Constellation (A-Train) (Stephens et al., 2002; Winker et al., 2010), researchers now have access to a near-continuous global record of vertically resolved observations of cloud and aerosol properties with nearly coincident observations from MODIS Aqua. Since launch, the CALIPSO lidar (the Cloud Aerosol 20 Lidar with Orthogonal Polarization, or CALIOP) has proven to be a valuable tool for developing and evaluating passive cloud retrievals (Ackerman et al., 2008; Delanoë; Hogan, 2010; Holz et al., 2008; Jin and Nasiri, 2013; Kahn et al., 2007). CALIOP

Resolving ice cloud optical thickness biases between CALIOP and MODIS

R. E. Holz et al.

Title Page

Abstract

Introduction

Conclusions

References

Tables

Figures



Back

Close

Full Screen / Esc

Printer-friendly Version

Interactive Discussion



can directly measure cloud-top height with sensitivities that are an order of magnitude greater than the passive retrievals, while the CALIOP depolarization and attenuated backscatter measurements provide vertically resolved cloud phase discrimination (Hu et al., 2009) for cloud layers up to a cumulative optical depth of about 3.

Ice Optical Thickness (IOT) has also proved to be one of the more challenging properties to retrieve from space-based passive sensor measurement. In particular, it is quite difficult to infer the microphysical and radiative properties of optically thin upper tropospheric ice clouds (cirrus) from observations made by passive space-borne instruments due to the tenuous nature, extensive spatial scales, complex particle shapes, and a wide range of particle sizes. There is a pressing need to conduct independent validation to examine systematic biases between MODIS Collection 5 (C5) and CALIOP Version 3 (V3) retrievals of tenuous IOT (< 3.0). To this end, we use a month of collocated A-Train observation to compare the aforementioned retrieval products. A factor of two bias is found between MODIS and CALIOP unconstrained retrievals (presented in Fig. 1), raising a major question regarding the utility of these data records to study ice cloud radiative processes. Here we seek to understand and resolve the CALIOP and MODIS IOT biases.

Both MODIS and CALIOP IOT retrievals require a priori information concerning the ice particle scattering properties that relate the measured reflectance (MODIS) or attenuated backscatter (CALIOP) to the cloud's IOT and potentially the effective particle size. MODIS ice cloud forward radiative calculations in the visible/near-infrared (VNIR) depend directly on the ice particle phase function assumption, and to a first order on the associated asymmetry parameter (g). For CALIOP, an assumed extinction-to-backscatter ratio is required for so-called "unconstrained" retrievals where the algorithm is unable to make reliable estimates of cirrus IOT by measuring the attenuated backscatter coefficients in some clear air region immediately below cloud base (Young and Vaughan, 2009). Because solar background signals greatly reduce the signal-to-noise ratio (SNR) of the CALIOP daytime measurements, the vast majority of CALIOP daytime IOT estimates are derived from unconstrained retrievals. Uncertainties in the

Resolving ice cloud optical thickness biases between CALIOP and MODIS

R. E. Holz et al.

Title Page

Abstract

Introduction

Conclusions

References

Tables

Figures



Back

Close

Full Screen / Esc

Printer-friendly Version

Interactive Discussion



Resolving ice cloud optical thickness biases between CALIOP and MODIS

R. E. Holz et al.

Title Page

Abstract

Introduction

Conclusions

References

Tables

Figures

◀

▶

◀

▶

Back

Close

Full Screen / Esc

Printer-friendly Version

Interactive Discussion



ice scattering property assumptions of either MODIS and/or CALIOP could account for the biases found in Fig. 1. As will be discussed, an infrared (IR) cirrus IOT retrieval is relatively insensitive to ice particle size and scattering details compared to MODIS and CALIOP VNIR measurements, and thus provides an independent means to assess thin to moderately optically thick cirrus retrievals (IOT \sim 0–3). In addition, an IR retrieval provides radiative closure with solar reflectance based MODIS IOT retrievals in the sense that consistency in the two retrieved IOTs also implies forward model consistency with the respective top-of-atmosphere (TOA) VNIR and IR observations.

Using the NASA-funded SSEC Atmosphere Product Evaluation and Test Element (PEATE), now re-named the Suomi-NPP Atmosphere Science Investigator Processing System (SIPS), the sensitivity of MODIS retrievals to ice single scattering properties are investigated by repeated analyses of collocated January 2010 CALIOP and MODIS observations using a variety of ice crystal habits (Yang et al., 2012) and size distributions. Based on comparisons against IR retrievals, the MODIS MYD06 Collection 6 (C6) ice cloud optical property algorithm uses a single habit – severely roughened aggregated columns (Yang et al., 2012) – instead of the size-dependent multi-habit model (Baum et al., 2005) used for C5. The MYD06 C6 results also compare well with a new CALIOP version that uses a modified (larger) extinction-to-backscattering ratio for unconstrained IOT retrievals.

2 Ice cloud optical thickness retrieval datasets

An overview of the relevant retrieval methodologies is presented here with a focus on the forward cloudy radiative transfer modeling assumptions and IR cirrus optical thickness retrievals developed specifically for this study.

2.1 IR retrievals and radiative closure

The MODIS channel suite includes a range of IR channels extending well into the CO₂ absorption region (13–15 μm). The calibration of the IR channels has been extensively validated and proven to have high accuracy with uncertainties less than 0.5 K across a broad temperature range (Tobin et al., 2006). For cirrus, the IR radiative transfer is dominated by absorption, and thus is less complex than for the VNIR retrieval. In this section we discuss the IR radiative transfer methodology that is used both to retrieve the IR IOT as well as evaluate the MODIS and CALIOP retrievals.

The goal of radiative closure study is to relate the differences in the CALIOP and MODIS retrieved IOT to the measured TOA channel radiance or Brightness Temperature (BT) in the MODIS 11 μm channel. To calculate the TOA cloudy radiances requires an accurate radiative transfer model, knowledge of the cloud boundaries, and well-characterized surface temperature/emissivity and atmospheric thermodynamic profiles. LBLDIS (Turner et al., 2003), a cloudy radiative transfer model, is used for this analysis. The model elegantly combines the clear sky Line By Line Radiative Transfer Model (LBLRTM) (Clough; Moncet, 1992) with the Discrete Ordinates Radiative Transfer (DISORT) (Stamnes et al., 1988), a proven and accurate cloudy radiative transfer model. The inputs required for LBLRTM are surface temperature and emissivity, vertically resolved temperature and water vapor profiles, and information regarding trace gas concentrations such as CO₂ and O₃. For this analysis the surface temperature and thermodynamic profiles are extracted from the NOAA Global Data Assimilation System (GDAS) files that provide profiles at 1° spatial resolution every 6 h. For each MODIS and CALIOP field of view (FOV), the closest (in both time and space) GDAS profile is selected. A fixed CO₂ concentration of 380 ppm and a climatological O₃ profile is used. Given these inputs LBLRTM is run on the selected FOV filtered using the collocated CALIOP V3 5 km layer products (described in Sect. 3). The results of the clear sky validation are discussed in Sect. 4.

Resolving ice cloud optical thickness biases between CALIOP and MODIS

R. E. Holz et al.

Title Page

Abstract

Introduction

Conclusions

References

Tables

Figures



Back

Close

Full Screen / Esc

Printer-friendly Version

Interactive Discussion



Resolving ice cloud optical thickness biases between CALIOP and MODIS

R. E. Holz et al.

Title Page

Abstract

Introduction

Conclusions

References

Tables

Figures



Back

Close

Full Screen / Esc

Printer-friendly Version

Interactive Discussion



This “reference” retrieval uses cloud boundary information from CALIOP coupled with the LBLDIS forward model and then retrieves the IR IOT using the MODIS 11 μm window channel observations that are coincident and collocated with CALIOP. A second method uses the spectral emissivity retrieved from the MODIS CO₂ emissive cloud-top pressure retrieval that is then related to the IOT and effective radius using a pre-computed lookup table (Heidinger et al., 2015). This method has the advantage of being computationally very efficient, not requiring the CALIOP cloud boundaries, and providing IOT for the entire MODIS swath. Both IR retrieval methods are discussed in more detail in the following sub-sections.

2.1.1 Combined MODIS IR window and CALIOP retrievals

A single channel IR window IOT retrieval was developed for this study using combined CALIOP and MODIS observations and the LBLDIS forward radiative transfer modeling discussed in the previous section. The method constrains the cloud boundaries using the collocated CALIOP 5 km layer products and uses surface and atmospheric temperatures information from GDAS. TOA radiances are simulated using LBLDIS with IOT retrieved by minimizing the measured MODIS channel 31 (11 μm) and calculated BT differences. The retrieval assumes the cloud extinction is evenly distributed in the vertical throughout the cloud. This simplification has the potential to bias the IOT for FOV where the IOT is distributed non-uniformly in the vertical (Maestri; Holz, 2009). The cloud geometric thickness is thus limited to no greater than 4 km to reduce IOT biases that can be introduced by non-homogeneous layers.

2.1.2 MODIS IR spectral emissivity retrievals

The MODIS C6 CO₂ slicing algorithm provides retrieved spectral emissivity for the 8.5, 11, and 12 μm channels (channels 29, 31, 32) that have sensitivity to both the IOT and effective radius. As described in Parol et al. (1991), β ratios can be approximated based on these emissivities and are related to the asymmetry parameter (g), single-scattering

albedo (ω_o), and extinction efficiency (Q_e) as follows:

$$\beta_{\lambda_1\lambda_2} = \frac{Q_{e,\lambda_1} (1 - \omega_{o,\lambda_1} g_{\lambda_1})}{Q_{e,\lambda_2} (1 - \omega_{o,\lambda_2} g_{\lambda_2})} \quad (1)$$

Thus β is the ratio of the scaled absorption extinction in two spectral channels (λ_1 and λ_2). The effective radius is first retrieved by matching simulated ice single-scattering calculations of $g(r)$, $\omega_o(r)$, and $Q_e(r)$, each integrated over the appropriate MODIS spectral response functions, to the retrieved MODIS β ratios. For this analysis the scattering properties of severely roughened aggregated columns (Yang et al., 2012) are used to be consistent with the MODIS C6 cloud optical property retrievals.

Using the effective radius to define $g(r)$, $\omega_o(r)$, and $Q_e(r)$, the extinction optical thickness is then retrieved by relating the 11 μm emissivity to the extinction optical thickness in the form (Van de Hulst, 1974):

$$\tau_{\text{vis}} = \frac{2}{Q_e} \left(\frac{\tau_{\text{abs}}}{(1 - \omega_o g)} \right), \quad (2)$$

where τ_{abs} is the IR absorption optical thickness and τ_{vis} is the extinction optical thickness at 532 nm. This derivation assumes that the ratio between the absorption and extinction optical thickness is a factor of 2 in the IR. Based on ice cloud single-scattering calculations (Yang et al., 2012) and assuming that the majority of ice clouds have an effective radius greater than 10 μm , this assumption is expected to have introduced no more than 10 % uncertainty. Heidinger et al. (2015) provides a more detailed discussion of the retrieval methodology. This approach can be applied without the need for the CALIOP cloud boundaries, and provides full swath IR IOT retrievals. We leverage this capability to investigate the MODIS IOT retrieval biases as a function of view angle.

Resolving ice cloud optical thickness biases between CALIOP and MODIS

R. E. Holz et al.

Title Page

Abstract

Introduction

Conclusions

References

Tables

Figures

◀

▶

◀

▶

Back

Close

Full Screen / Esc

Printer-friendly Version

Interactive Discussion



thermal IR portions of the spectrum. Spatial resolution is 250 m in two VNIR channels, 500 m in 5 VIS/SWIR channels, and 1 km in the remaining channels.

The MODIS cloud optical/microphysical property algorithm is used to generate a single cloud product designated by the NASA Earth science data type (ESDT) names MOD06 and MYD06 for Terra and Aqua MODIS, respectively (hereafter referred to as MYD06 since the algorithms are essentially identical and this study is focused on MODIS Aqua observations). For daytime measurements, the 1 km cloud retrieval algorithm uses multiple spectral channels (primarily six VNIR, SWIR and MWIR channels, as well as several thermal channels) to simultaneously retrieve cloud optical thickness, effective radius (and derived water path) and thermodynamic phase for liquid and ice phase clouds. In addition to the 1 km MODIS Level-1B calibrated radiance product, the algorithm requires the following input: MODIS cloud mask (MYD35) including 250 m mask information (Ackerman et al., 1998), the cloud-top pressure portion of MYD06 (Ackerman et al., 2008; Holz et al., 2008), and a variety of ancillary datasets. Heritage algorithm work is discussed in King et al. (2003); Nakajima and King (1990); Platnick and Twomey (1994); Platnick et al. (2001, 2003).

C5 algorithm-related publications include ice radiative models (Ackerman et al., 2008; Baum et al., 2005; Yang et al., 2007) multilayer detection (Wind et al., 2010), Clear Sky Restoral filtering (Pincus et al., 2012; Zhang and Platnick, 2011), pixel-level uncertainties (Platnick et al., 2004), and L3 global gridded statistics (King et al., 2013). An online list of the recent C6 algorithm updates is available from the MODIS Atmosphere Team web site (Platnick, 2014). The most relevant update for the current discussion is the adoption of new ice cloud radiative models having an overall smaller asymmetry parameter, as will be discussed in Sect. 5.1. Note for consistency with the spherical droplet definition, as well as for use in deriving ice water path, the effective radius of a non-spherical ice particle is defined as 3/4 times the ratio of the average volume of the size distribution to the average cross sectional area (Yang et al., 2007).

Resolving ice cloud optical thickness biases between CALIOP and MODIS

R. E. Holz et al.

Title Page

Abstract

Introduction

Conclusions

References

Tables

Figures



Back

Close

Full Screen / Esc

Printer-friendly Version

Interactive Discussion



3 Collocation and the merged dataset

In this section we present the methods used to collocate and merge the CALIOP and MODIS observations providing the foundation for the inter-comparisons and analysis presented in the results of Sect. 4.

The analysis is based on one month (January 2010) of physically collocated CALIOP and MODIS observations. MODIS is an imaging radiometer while CALIOP is a near-nadir viewing lidar. Because each instrument has a unique viewing geometry with different spatial resolutions, accurate inter-comparisons require collocating the observation FOVs. This analysis uses tools that provide computationally efficient and accurate collocation (Nagle and Holz, 2009). The methodology defines master and follower instruments, with the master typically being the larger FOV and the follower FOV collocated within the master footprint. In this investigation MODIS is defined as the master with CALIOP the follower. The MODIS spatial resolution can be approximated as a rectangular box with a 1×2 km resolution at nadir. The CALIOP IOT retrieval can be performed over horizontal averaging distances ranging from 5 to 80 km, depending on the magnitude of the cloud signal relative to the background noise (Yongxiang et al., 2007). The CALIOP surface footprint is therefore approximated as an 80 m wide swath with the along-track length depending on the amount of spatial averaging. The majority of observations used in this analysis are the 5 km averaged IOT. A more detailed description of the CALIOP and MODIS collocation is presented in Holz et al. (2008).

Leveraging the UW Atmospheric Science Investigator-led Processing System (SIPs) processing capabilities, a month of collocated MODIS and CALIOP collocated observations were processed using the CALIOP and MODIS IOT retrievals with the only difference being incremental changes to the ice cloud parameterizations used in the retrieval algorithms. This approach isolates the impact of the parameterization changes and/or algorithm modifications and provides a direct assessment of the changes in IOT.

Resolving ice cloud optical thickness biases between CALIOP and MODIS

R. E. Holz et al.

Title Page

Abstract

Introduction

Conclusions

References

Tables

Figures



Back

Close

Full Screen / Esc

Printer-friendly Version

Interactive Discussion



Resolving ice cloud optical thickness biases between CALIOP and MODIS

R. E. Holz et al.

Title Page

Abstract

Introduction

Conclusions

References

Tables

Figures



Back

Close

Full Screen / Esc

Printer-friendly Version

Interactive Discussion



To put the biases into a radiative context, the cloudy IR TOA fluxes are computed for each collocated FOV using RRTM. The calculations use the CALIOP cloud boundaries, the surface and atmospheric profiles from GDAS, and the MODIS retrieved effective radius. For each collocated FOV two RRTM calculations are computed with the only difference being the IOT used (MODIS or CALIOP) with the results presented in Fig. 2b. The mean TOA flux difference between MODIS and CALIOP unconstrained retrievals is $+23 \text{ W m}^{-2}$ with a standard deviation of 21 W m^{-2} . For the tenuous cirrus being investigated, the sensitivity of the TOA flux to IOT is primarily driven by the thermal contrast between the surface and the mean emitting temperature of the cloud. The very large differences in the wings of the distribution in Fig. 1b occur primarily near the tropics where the thermal contrast is greatest between the cloud and the surface. For this region TOA differences as large as 50 W m^{-2} are found in Fig. 2b.

5 IR retrievals as a reference optical thickness

Because the sensitivity of IR IOT retrievals to ice crystal habit selection is minimal, these retrievals provide an independent means to evaluate the CALIOP and MODIS solar reflectance retrievals. As discussed in Sect. 2, the main sources of uncertainty in the IR IOT originate from characterizing the surface temperature and having an accurate determination of the cloud emitting temperature. To reduce the surface temperature uncertainty, the results of this section are restricted to non-polar ($\pm 60^\circ$) ocean-only cases.

The comparisons with IR window IOT retrievals shown in Fig. 3 reveal biases in both the MODIS (a) and daytime CALIOP unconstrained (b) retrievals (high and low, respectively) that are consistent with the radiative closure results presented in Fig. 2. The magnitude of the bias relative to the IR is approximately +40% for MODIS. For CALIOP there is a non-linear dependence between the IOT and the negative bias relative to the IR, with the bias increasing substantially for IR IOTs greater than unity; the CALIOP results are discussed further in Sect. 5.2.

Both results led to the decision to use the severely roughened aggregated column radiative model for the MODIS C6 cloud optical/microphysical property retrievals.

Figure 8 shows an example of ice cloud retrievals for C5 and C6 for typhoon Fung-Wong. The typhoon was located south of Taiwan at the time of the MODIS Aqua data granule acquisition on 20 September 2014 (05:30 UTC). The C5 and C6 ice (cool colors) and liquid (warm colors) cloud optical thickness retrievals are shown in the middle and right panels, respectively. In addition to ice radiative model differences, MYD06 C5 and C6 have different schemes for the cloud thermodynamic phase yielding different ice and liquid phase pixel populations, though the optical thickness spatial patterns are similar for regions having the same phase. Because of the different phase assignments made by these two scheme, quantifying ice model retrieval sensitivities requires the comparisons be restricted to only those pixels for which both algorithms generate successful retrievals that identify identical cloud phases. With this pixel filtering, the left panel of Fig. 8b shows the normalized IOT distribution for the optical thickness range of the plot. The C6 IOT mode is roughly 27 % smaller than the C5 mode, while the mean is decreased by about 15 %, from 4.16 for C5 to 3.55 for C6. The 2.1 μm ice cloud effective particle radius retrievals are shown in the right panel, with the C6 mode and mean both increasing by about 4 μm (+15 %) for C6 relative to C5.

5.2 MODIS C6 model selection methodology

The MODIS IOT retrieval depends strongly on assumed ice scattering properties that are needed to relate the measured reflectance to the retrieved IOT. The MODIS C5 retrieval used empirically derived habit and size distributions with asymmetry parameters ranging between 0.79 and 0.88, depending on the ice cloud effective radius (Baum et al., 2005). By conducting an infrared closure analysis, we have shown that the C5 parameterization is not representative of the globally averaged ice scattering properties. More recent investigations of the ice cloud asymmetry parameter suggest that most ice clouds have values around 0.75 in the visible spectrum. Additionally, use of the C5 ice cloud radiative model results in MODIS retrieval biases are strongly de-

Resolving ice cloud optical thickness biases between CALIOP and MODIS

R. E. Holz et al.

Title Page

Abstract

Introduction

Conclusions

References

Tables

Figures



Back

Close

Full Screen / Esc

Printer-friendly Version

Interactive Discussion



assessing the CALIOP and MODIS IOT clearly demonstrates that both retrievals have significant biases, but in opposite directions: MODIS C5 systematically overestimates IOT while CALIOP V3 systematically underestimates IOT.

The decision to use the single severely roughened aggregate column habit as the MODIS C6 ice cloud radiative model was made solely to achieve closure with IR retrievals in a global sense. Our use of this model for this purpose does not imply that it is a suitable microphysical model for use in understanding ice particle physical processes, e.g., size distribution evolution, fall speed distribution, etc. Furthermore, the IR comparisons were done in conjunction with collocated CALIOP observations that allow for the filtering of multi-layer ice phase clouds from the statistical study; The data set used here is clearly a subset of actual scenes and so may not be reflective of the full distribution of ice clouds observed by the sensors. Finally, it is recognized that using a fixed ice radiative model for global retrievals is only meaningful in a climatological sense and may be expected to breakdown in instantaneous and/or regional studies.

The severely roughened aggregated column model adopted for the MODIS C6 ice cloud algorithm has a fixed aspect ratio with an asymmetry parameter of about 0.75 in the visible for all effective sizes. This produces results that are quite consistent with those generated using the Inhomogeneous Hexagonal Mono-crystal (IHM) model derived by Labonnote et al. (2001) (asymmetry parameter of about 0.77) that provided a good match with observed POLDER view angle-dependent VNIR reflectance. Other studies have also suggested that featureless (i.e., smooth) phase functions indicative of roughened or highly asymmetric aggregated habits with relatively small asymmetry parameters are needed to match aircraft and satellite observations (e.g., Baran et al., 2001; Labonnote et al., 2000; van Diedenhoven et al., 2013).

The Generalized Habit Model (GHM) (Baum et al., 2010) was also tested but did not the same level of radiative closure with the IR IOT retrievals compared to the severely roughened aggregated columns (comparison shown in Fig. 7a). While there was an improvement with respect to the C5 ice model (comparison shown in Fig. 3a), the GHM model resulted in IOT retrievals that were still significantly larger than the IR

Resolving ice cloud optical thickness biases between CALIOP and MODIS

R. E. Holz et al.

Title Page

Abstract

Introduction

Conclusions

References

Tables

Figures



Back

Close

Full Screen / Esc

Printer-friendly Version

Interactive Discussion



Resolving ice cloud optical thickness biases between CALIOP and MODIS

R. E. Holz et al.

Title Page

Abstract

Introduction

Conclusions

References

Tables

Figures



Back

Close

Full Screen / Esc

Printer-friendly Version

Interactive Discussion



because of larger asymmetry parameters in the visible relative to the severely roughened aggregated column model (about 0.77 at an effective radius of 5 μm up to 0.82 at 60 μm). Cole et al. (2012) also tested the GHM as well as single habit models from Yang et al. (2003, 2012) against POLDER polarized and total reflectance observations across a range of scattering angles. Polarized angular observations agreed well with a severely roughened version of the GHM. However, it was concluded that there was no single habit/model that is best in all respects for the reflectance (derived spherical albedo) consistency tests, though the severely roughened aggregated column model was not included in the analysis. Similarly, Baran and Labonnote (2007) also noted that though the IHM model provided good consistency with POLDER directional reflectance distributions, it was less successful in matching the angular distribution of polarized reflectances. Due to vertical size stratification in ice clouds it is possible that different models are needed to match polarized observations (weighted towards the uppermost portion of the cloud-top) with total reflectance observations (weighted deeper into the cloud), e.g., Platnick (2000) and Zhang et al. (2010). Given that MODIS retrievals are based on total reflectance, it is expected that directional reflectance consistency with POLDER is the more relevant metric. Further, the study of Zhang et al. (2010) shows there is little difference between IOT retrieved from reflectance and IR observations for the model case study considered. Fauchez et al. (2014) demonstrated that for 1 km IR observations, sensitivities to 3-D effects are limited to horizontal heterogeneity (plane-parallel approximation or PPA bias) and the effect of vertical heterogeneity is small. Though more extensive heterogeneity studies are needed, these studies do suggest the utility of using IR IOT retrievals to assess MODIS reflectance-based ice radiative models. Finally, we note that recent comparisons have demonstrated consistency between Aqua MODIS C6 IOT retrievals and those from AIRS Version 6 (Kahn, 2015).

For CALIOP it is found that the bias relative to the IR for the V3 IOT retrievals depends on the retrieval method used. While CALIOP can make direct measurements of the effective two-way transmittance of the layer, the retrieved optical thickness depends only on an estimate of the multiple scattering factor and the accuracy of the molecu-

Resolving ice cloud optical thickness biases between CALIOP and MODIS

R. E. Holz et al.

Title Page

Abstract

Introduction

Conclusions

References

Tables

Figures



Back

Close

Full Screen / Esc

Printer-friendly Version

Interactive Discussion



lar attenuated backscatter profile (calculated from a temperature and pressure profile using Rayleigh scattering theory). However, daytime solar background noise limits the applicability of this constrained retrieval technique to mostly nighttime observations, thus prohibiting direct comparisons to the MODIS daytime optical retrievals. For the constrained retrieval we find good agreement with the IR radiative closure (Fig. 2) and the IR IOT in Fig. 9. However, the majority of the daytime CALIOP retrievals use the unconstrained method that requires an a priori specification of the cloud extinction-to-backscatter ratio. It is these unconstrained retrievals that are directly compared to the MODIS C5 IOT in Fig. 1 and to the IR in Fig. 2 and Fig. 3. The CALIOP V3 unconstrained IOT retrievals show a significant low bias relative to both the IR and the constrained CALIOP retrievals. Since both CALIOP methods assume an identical multiple scattering correction, this suggests that the default lidar ratio (25 sr) used in the V3 CALIOP unconstrained retrievals is too low. As part of this investigation the CALIOP algorithm team processed a month of retrievals using a lidar ratio of 32 sr for the unconstrained retrievals with results presented in Fig. 7b. It is important to note that the selection of a lidar ratio of 32 sr was not based on the IR inter-comparison studies, but instead was derived from independent analyses of the nighttime constrained retrievals conducted by the CALIOP algorithm team in order to improve the accuracy of the CALIOP unconstrained retrievals and increase the consistency of IOTs reported by the constrained and unconstrained retrievals.

Acknowledgements. We would like to acknowledge the NASA University of Wisconsin Atmospheric PEATE/SIPS that provide the processing and data accessed needed to conduct this research. We would also like to thank the CALIOP and MODIS algorithm teams for their support. This research was funded by NASA grant NNX15AG12G and NASA Langley Contract SSAI Task A-014 E-001D.

References

- Ackerman, S. A., Holz, R. E., Frey, R., Eloranta, E. W., Maddux, B., and McGill, M. J.: Cloud detection with MODIS: Part II validation, *J. Atmos. Ocean. Tech.*, 25, 1073–1086, 2008.
- Baran, A. J. and Labonnote, L. C.: A self-consistent scattering model for cirrus, I: the solar region, *Q. J. Roy. Meteor. Soc.*, 133, 1899–1912, 2007.
- Baran, A. J., Francis, P. N., Labonnote, L. C., and Doutriaux-Boucher, M.: A scattering phase function for ice cloud: tests of applicability using aircraft and satellite multi-angle multi-wavelength radiance measurements of cirrus, *Q. J. Roy. Meteor. Soc.*, 127, 2395–2416, 2001.
- Baum, B. A., Yang, P., Heymsfield, A. J., Platnick, S., King, M. D., Hu, Y.-X., and Bedka, S. T.: Bulk scattering properties for the remote sensing of ice clouds, Part II: Narrowband models, *J. Appl. Meteorol.*, 44, 1896–1911, 2005.
- Baum, B. A., Yang, P., Heymsfield, A. J., Platnick, S., King, M. D., Hu, Y.-X., and Bedka, S. T.: Improvements in shortwave bulk scattering and absorption models for the remote sensing of ice clouds, *J. Appl. Meteorol. Clim.*, 50, 1037–1056, 2010.
- Clough, S. A. and Moncet, J. L.: Line by line calculations of atmospheric fluxes and cooling rates: application to carbon dioxide, ozone, methane, nitrous oxide, and the halocarbons, *J. Geophys. Res.*, 97, 761–785, 1992.
- Cole, B. H., Yang, P., Baum, B. A., Riedi, J., Labonnote, L. C., Thieuleux, F., and Platnick, S.: Comparison of PARASOL observations with polarized reflectances simulated using different ice habit mixtures, *J. Appl. Meteorol. Clim.*, 52, 186–196, 2012.
- Delanoë, J. and Hogan, R. J.: Combined CloudSat-CALIPSO-MODIS retrievals of the properties of ice clouds, *J. Geophys. Res.-Atmos.*, 115, 2156–2202, 2010.
- Fauchez, T., Cornet, C., Szczap, F., Dubuisson, P., and Rosambert, T.: Impact of cirrus clouds heterogeneities on top-of-atmosphere thermal infrared radiation, *Atmos. Chem. Phys.*, 14, 5599–5615, doi:10.5194/acp-14-5599-2014, 2014.
- Fu, Q., Carlin, B., and Mace, G.: Cirrus horizontal inhomogeneity and OLR bias, *Geophys. Res. Lett.*, 27, 3341–3344, 2000.
- Garnier, A., Pelon, J., Vaughan, M. A., Winker, D. M., Trepte, C. R., and Dubuisson, P.: Lidar multiple scattering factors inferred from CALIPSO lidar and IIR retrievals of semi-transparent cirrus cloud optical depths over oceans, *Atmos. Meas. Tech.*, 8, 2759–2774, doi:10.5194/amt-8-2759-2015, 2015.

Resolving ice cloud optical thickness biases between CALIOP and MODIS

R. E. Holz et al.

Title Page

Abstract

Introduction

Conclusions

References

Tables

Figures



Back

Close

Full Screen / Esc

Printer-friendly Version

Interactive Discussion



Resolving ice cloud optical thickness biases between CALIOP and MODIS

R. E. Holz et al.

Title Page

Abstract

Introduction

Conclusions

References

Tables

Figures



Back

Close

Full Screen / Esc

Printer-friendly Version

Interactive Discussion



- Heidinger, A. K., Foster, M. J., Walther, A., and Zhao, X.: The pathfinder atmospheres-extended AVHRR climate dataset, *B. Am. Meteorol. Soc.*, 95, 909–922, 2013.
- Heidinger, A., Li, Y., Baum, B., Holz, R., Platnick, S., and Yang, P.: Retrieval of cirrus cloud optical depth under day and night conditions from MODIS collection 6 cloud property data, *Remote Sens.*, 7, 7257–7271, 2015.
- Holz, R. E.: Measurement cirrus backscatter phase functions using a high spectral resolution lidar, Atmospheric and Oceanic Sciences, University of Wisconsin-Madison, Madison, WI, 67 p., 2002.
- Holz, R. E., Ackerman, S. A., Nagel, F. W., Frey, R., Dutcher, S., Kuehn, R. E., Vaughan, M. A., and Baum, B. A.: Global MODIS cloud detection and height evaluated using CALIOP, *J. Geophys. Res.*, doi:10.1029/2008JD009837, 2008.
- Hu, Y., Winker, D., Vaughan, M., Lin, B., Omar, A., Trepte, C., Flittner, D., Yang, P., Nasiri, S. L., Baum, B., Holz, R., Sun, W., Liu, Z., Wang, Z., Young, S., Stamnes, K., Huang, J., and Kuehn, R.: CALIPSO/CALIOP cloud phase discrimination algorithm, *J. Atmos. Ocean. Tech.*, 26, 2293–2309, 2009.
- Hunt, W. H., Winker, D. M., Vaughan, M. A., Powell, K. A., Lucker, P. L., and Weimer, C.: CALIPSO lidar description and performance assessment, *J. Atmos. Ocean. Tech.*, 26, 1214–1228, 2009.
- Jiang, J. H., Su, H., Zhai, C., Perun, V. S., Del Genio, A., Nazarenko, L. S., Donner, L. J., Horowitz, L., Seman, C., Cole, J., Gettelman, A., Ringer, M. A., Rotstayn, L., Jeffrey, S., Wu, T., Brient, F., Dufresne, J.-L., Kawai, H., Koshiro, T., Watanabe, M., Lécuyer, T. S., Volodin, E. M., Iversen, T., Drange, H., Mesquita, M. D. S., Read, W. G., Waters, J. W., Tian, B., Teixeira, J., and Stephens, G. L.: Evaluation of cloud and water vapor simulations in CMIP5 climate models using NASA “A-Train” satellite observations, *J. Geophys. Res.-Atmos.*, 117, 2156–2202, 2012.
- Jin, H. and Nasiri, S. L.: Evaluation of AIRS cloud-thermodynamic-phase determination with CALIPSO, *J. Appl. Meteorol. Clim.*, 53, 1012–1027, 2013.
- Josset, D., Pelon, J., Garnier, A., Hu, Y., Vaughan, M., Zhai, P.-W., Kuehn, R., and Lucker, P.: Cirrus optical depth and lidar ratio retrieval from combined CALIPSO-CloudSat observations using ocean surface echo, *J. Geophys. Res.-Atmos.*, 117, 2156–2202, 2012.
- Kahn, B. H.: Pixel-scale assessment and uncertainty analysis of AIRS and MODIS ice cloud optical thickness and effective radius, *J. Geophys. Res.*, submitted, 2015.

Resolving ice cloud optical thickness biases between CALIOP and MODIS

R. E. Holz et al.

[Title Page](#)[Abstract](#)[Introduction](#)[Conclusions](#)[References](#)[Tables](#)[Figures](#)[Back](#)[Close](#)[Full Screen / Esc](#)[Printer-friendly Version](#)[Interactive Discussion](#)

- Kahn, B. H., Chahine, M. T., Stephens, G. L., Mace, G. G., Marchand, R. T., Wang, Z., Barnett, C. D., Eldering, A., Holz, R. E., Kuehn, R. E., and Vane, D. G.: Cloud type comparisons of AIRS, CloudSat, and CALIPSO cloud height and amount, *Atmos. Chem. Phys.*, 8, 1231–1248, doi:10.5194/acp-8-1231-2008, 2008.
- 5 King, M. D., Platnick, S., Menzel, W. P., Ackerman, S. A., and Hubanks, P. A.: Cloud and aerosol properties, precipitable water, and profiles of temperature and humidity from MODIS, *IEEE T. Geosci. Remote*, 41, 442–458, 2003.
- King, M. D., Platnick, S., Menzel, W. P., Ackerman, S. A., and Hubanks, P. A.: Spatial and temporal distribution of clouds observed by MODIS onboard the Terra and Aqua Satellites, *IEEE T. Geosci. Remote*, 51, 3826–3852, 2013.
- 10 Labonnote, L. C., Brogniez, G., Doutriaux-Boucher, M., Buriez, J.-C., Gayet, J.-F., and Chepfer, H.: Modeling of light scattering in cirrus clouds with inhomogeneous hexagonal monocrystals, comparison with in-situ and ADEOS-POLDER measurements, *Geophys. Res. Lett.*, 27, 113–116, 2000.
- 15 Labonnote, L. C., Brogniez, G., Buriez, J.-C., Doutriaux-Boucher, M., Gayet, J.-F., and Macke, A.: Polarized light scattering by inhomogeneous hexagonal monocrystals: validation with ADEOS-POLDER measurements, *J. Geophys. Res.-Atmos.*, 106, 12139–12153, 2001.
- Liu, Z., Vaughan, M., Winker, D., Kittaka, C., Getzewich, B., Kuehn, R., Omar, A., Powell, K., Trepte, C., and Hostetler, C.: The CALIPSO lidar cloud and aerosol discrimination: version 2 algorithm and initial assessment of performance, *J. Atmos. Ocean. Tech.*, 26, 1198–1213, 2009.
- 20 Maestri, T. and Holz, R. E.: Retrieval of cloud optical properties from multiple infrared hyperspectral measurements: a methodology based on a line-by-line multiple-scattering code, *IEEE T. Geosci. Remote*, 47, 2413–2426, 2009.
- 25 Mlawer, E. J., Taubman, S. J., Brown, P. D., Iacono, M. J., and Clough, S. A.: Radiative transfer for inhomogeneous atmospheres: RRTM, a validated correlated-k model for the longwave, *J. Geophys. Res.*, 102, 2156–2202, 1997.
- Nagle, F. W. and Holz, R. E.: Computationally efficient methods of collocating satellite, aircraft, and ground observations, *J. Atmos. Ocean. Tech.*, 26, 1585–1595, 2009.
- 30 Nakajima, T. and King, M. D.: Determination of the optical thickness and effective particle radius of clouds from reflected solar radiation measurements, Part I: Theory, *J. Atmos. Sci.*, 47, 1878–1893, 1990.

Resolving ice cloud optical thickness biases between CALIOP and MODIS

R. E. Holz et al.

Title Page

Abstract

Introduction

Conclusions

References

Tables

Figures



Back

Close

Full Screen / Esc

Printer-friendly Version

Interactive Discussion



Parol, F., Buriez, J. C., Brogniez, G., and Fouquart, Y.: Information content of AVHRR channels 4 and 5 with respect to the effective radius of cirrus cloud particles, *J. Appl. Meteorol.*, 30, 973–984, 1991.

Pincus, R., Platnick, S., Ackerman, S. A., Hemler, R. S., and Patrick Hofmann, R. J.: Reconciling simulated and observed views of clouds: MODIS, ISCCP, and the limits of instrument simulators, *J. Climate*, 25, 4699–4720, 2012.

Platnick, S.: Vertical photon transport in cloud remote sensing problems, *J. Geophys. Res.-Atmos.*, 105, 22919–22935, 2000.

Platnick, S.: MODIS Cloud Optical Properties: User Guide for the Collection 6 Level-2 MOD06/MYD06 Product and Associated Level-3 Datasets, 141 p., 2014.

Platnick, S. and Twomey, S.: Determining the susceptibility of cloud albedo to changes in droplet concentration with the advanced very high resolution radiometer, *J. Appl. Meteorol.*, 33, 334–347, 1994.

Platnick, S., Li, J. Y., King, M. D., Gerber, H., and Hobbs P. V.: A solar reflectance method for retrieving the optical thickness and droplet size of liquid water clouds over snow and ice surfaces, *J. Geophys. Res.-Atmos.*, 106, 15185–15199, 2001.

Platnick, S., King, M. D., Ackerman, S. A., Menzel, W. P., Baum, B. A., Riedi, J. C., and Frey, R. A.: The MODIS cloud products: algorithms and examples from Terra, *IEEE T. Geosci. Remote*, 41, 459, doi:10.1109/TGRS.2002.808301, 2003.

Powell, K. A., Hostetler, C. A., Vaughan, M. A., Lee, K.-P., Trepte, C. R., Rogers, R. R., Winker, D. M., Liu, Z., Kuehn, R. E., Hunt, W. H., and Young, S. A.: CALIPSO lidar calibration algorithms, Part I: Nighttime 532 nm parallel channel and 532 nm perpendicular channel, *J. Atmos. Ocean. Tech.*, 26, 2015–2033, 2009.

Rossow, W. B.: Use of operational satellite data for study of clouds and radiation in climate, *Global Planet. Change*, 90, 33–39, 1991.

Rossow, W. B. and Schiffer, R. A.: Advances in understanding clouds from ISCCP, *B. Am. Meteorol. Soc.*, 80, 2261–2287, 1999.

Sassen, K. C. and Jennifer, M.: A midlatitude cirrus cloud climatology from the facility for atmospheric remote sensing, Part III: Radiative properties, *J. Atmos. Sci.*, 58, 2113–2127, 2001.

Stamnes, K., Tsay, S., Wiscombe, W. J., and Jayaweera, K.: Numerically stable algorithm for discrete-ordinate-method radiative transfer in multiple scattering and emitting layered media, *Appl. Optics*, 27, 2502–2509, 1988.

Resolving ice cloud optical thickness biases between CALIOP and MODIS

R. E. Holz et al.

Title Page

Abstract

Introduction

Conclusions

References

Tables

Figures



Back

Close

Full Screen / Esc

Printer-friendly Version

Interactive Discussion



Stephens, G. L., Vane, D. G., Boain, R. J., Mace, G. G., Sassen, K., Wang, Z. E., Illingworth, A. J., O'Connor, E. J., Rossow, W. B., Durden, S. L., Miller, S. D., Austin, R. T., Benedetti, A., Mitrescu, C., and Team, C. S.: The cloudsat mission and the a-train – a new dimension of space-based observations of clouds and precipitation, *B. Am. Meteorol. Soc.*, 83, 1771–1790, 2002.

Tobin, D. C., Revercomb, H. E., Moeller, C. C., and Pagano, T. S.: Use of atmospheric infrared sounder high spectral resolution spectra to assess the calibration of moderate resolution imaging spectroradiometer on EOS Aqua, *J. Geophys. Res.*, 111, D09S05, doi:10.1029/2005JD006095, 2006.

Turner, D. D., Ackerman, S. A., Baum, B. A., Revercomb, H. E., and Yang, P.: Cloud phase determination using ground-based AERI observations at SHEBA, *J. Appl. Meteorol.*, 42, 701–715, 2003.

Van de Hulst, H. C.: The spherical albedo of a planet covered with a homogeneous cloud layer, *Astron. Astrophys.*, 35, 209–214, 1974.

van Diedenhoven, B., Cairns, B., Fridlind, A. M., Ackerman, A. S., and Garrett, T. J.: Remote sensing of ice crystal asymmetry parameter using multi-directional polarization measurements – Part 2: Application to the research scanning polarimeter, *Atmos. Chem. Phys.*, 13, 3185–3203, doi:10.5194/acp-13-3185-2013, 2013.

Vaughan, M. A., Winker, D., and Powell, K. A.: CALIOP Algorithm Theoretical Basis Document, Part 2: Feature Detection and Layer Properties Algorithms, N. L. R. Center, 1–87, Ed., 2005.

Vaughan, M. A., Powell, K. A., Winker, D. M., Hostetler, C. A., Kuehn, R. E., Hunt, W. H., Getzewich, B. J., Young, S. A., Liu, Z., and McGill, M. J.: Fully automated detection of cloud and aerosol layers in the CALIPSO lidar measurements, *J. Atmos. Ocean. Tech.*, 26, 2034–2050, 2009.

Wind, G., Platnick, S., King, M. D., Hubanks, P. A., Pavolonis, M. J., Heidinger, A. K., Yang, P., and Baum, B. A.: Multilayer cloud detection with the MODIS near-infrared water vapor absorption band, *J. Appl. Meteorol. Clim.*, 49, 2315–2333, 2010.

Winker, D.: Accounting for multiple scattering in retrievals from space lidar, *SPIE*, 5059, 128–139, 2003.

Winker, D. M., Pelon, J., Coakley, J. A., Ackerman, S. A., Charlson, R. J., Colarco, P. R., Flamant, P., Fu, Q., Hoff, R. M., Kittaka, C., Kubar, T. L., Le Treut, H., McCormick, M. P., Mégie, G., Poole, L., Powell, K., Trepte, C., Vaughan, M. A., and Wielicki, B. A.: The CALIPSO

Resolving ice cloud optical thickness biases between CALIOP and MODIS

R. E. Holz et al.

Title Page

Abstract

Introduction

Conclusions

References

Tables

Figures



Back

Close

Full Screen / Esc

Printer-friendly Version

Interactive Discussion



mission: a global 3-D view of aerosols and clouds, *B. Am. Meteorol. Soc.*, 91, 1211–1229, 2010.

Wylie, D. P. and Menzel, W. P.: Eight years of high cloud statistics using HIRS, *J. Climate*, 12, 170–184, 1999.

5 Yang, P., Hu, Y. X., Winker, D. M., Zhao, J., Hostetler, C. A., Poole, L., Baum, B. A., Mishchenko, M. I., and Reichardt, J.: Enhanced lidar backscattering by quasi-horizontally oriented ice crystal plates in cirrus clouds, *J. Quant. Spectrosc. Ra.*, 79–80, 1139–1157, 2003.

10 Yang, P., Lei, Z., Hong, G., Nasiri, S. L., Baum, B. A., Huang, H. L., King, M. D., and Platnick, S.: Differences between collection 4 and 5 MODIS ice cloud optical/microphysical products and their impact on radiative forcing simulations, *IEEE T. Geosci. Remote*, 45, 2886–2899, 2007.

Yang, P., Bi, L., Baum, B. A., Liou, K.-N., Kattawar, G. W., Mishchenko, M. I., and Cole, B.: Spectrally consistent scattering, absorption, and polarization properties of atmospheric ice crystals at wavelengths from 0.2 to 100 μm , *J. Atmos. Sci.*, 70, 330–347, 2012.

15 Yongxiang, H., Vaughan, M., Liu, Z., Powell, K., and Rodier, S.: Retrieving optical depths and lidar ratios for transparent layers above opaque water clouds from CALIPSO lidar measurements, *IEEE Geosci. Remote S.*, 4, 523–526, 2007.

Yorks, J. E., Hlavka, D. L., Hart, W. D., and McGill, M. J.: Statistics of cloud optical properties from airborne lidar measurements, *J. Atmos. Ocean. Tech.*, 28, 869–883, 2011.

20 Young, S. A.: Analysis of lidar backscatter profiles in optically thin clouds, *Appl. Optics*, 34, 7019–7031, 1995.

Young, S. A. and Vaughan, M. A.: The retrieval of profiles of particulate extinction from cloud-aerosol lidar infrared pathfinder satellite observations (CALIPSO) data: algorithm description, *J. Atmos. Ocean. Tech.*, 26, 1105–1119, 2009.

25 Zhang, Z. and Platnick, S.: An assessment of differences between cloud effective particle radius retrievals for marine water clouds from three MODIS spectral bands, *J. Geophys. Res.-Atmos.*, 116, D20215, doi:10.1029/2011JD016216, 2011.

30 Zhang, Z., Platnick, S., Yang, P., Heidinger, A. K., and Comstock, J. M.: Effects of ice particle size vertical inhomogeneity on the passive remote sensing of ice clouds, *J. Geophys. Res.-Atmos.*, 115, D17203, doi:10.1029/2010JD013835, 2010.

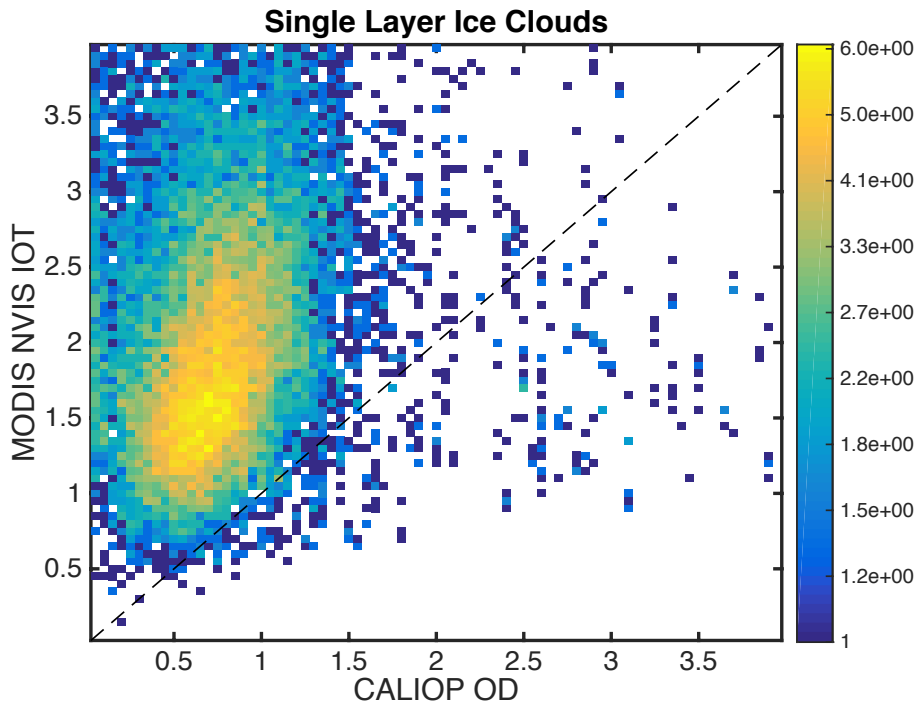


Figure 1. A two dimensional histogram comparing MODIS C5 and CALIOP V3 single layer ice cloud daytime optical thickness retrievals for January 2010 (ocean surfaces, $\pm 60^\circ$ latitude). Notice the color scale is logarithmic.

Resolving ice cloud optical thickness biases between CALIOP and MODIS

R. E. Holz et al.

Title Page	
Abstract	Introduction
Conclusions	References
Tables	Figures
◀	▶
◀	▶
Back	Close
Full Screen / Esc	
Printer-friendly Version	
Interactive Discussion	



Resolving ice cloud optical thickness biases between CALIOP and MODIS

R. E. Holz et al.

Title Page

Abstract

Introduction

Conclusions

References

Tables

Figures



Back

Close

Full Screen / Esc

Printer-friendly Version

Interactive Discussion

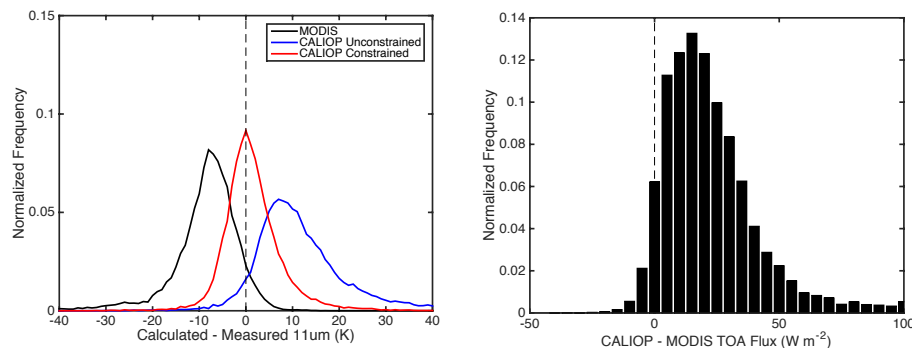


Figure 2. This figure presents the radiative closure results **(a)** for 1 month (January 2010) of collocated single layer ice cloud observations using LBLRTM and DISORT to calculate the TOA 11 μm radiance that are compared to MODIS channel 31 observations. The only difference in the calculations is the IOT retrieval method. The differences in TOA fluxes resulting from using the MODIS or CALIOP daytime IOT retrievals in the calculation are presented the right histogram **(b)**.

Resolving ice cloud optical thickness biases between CALIOP and MODIS

R. E. Holz et al.

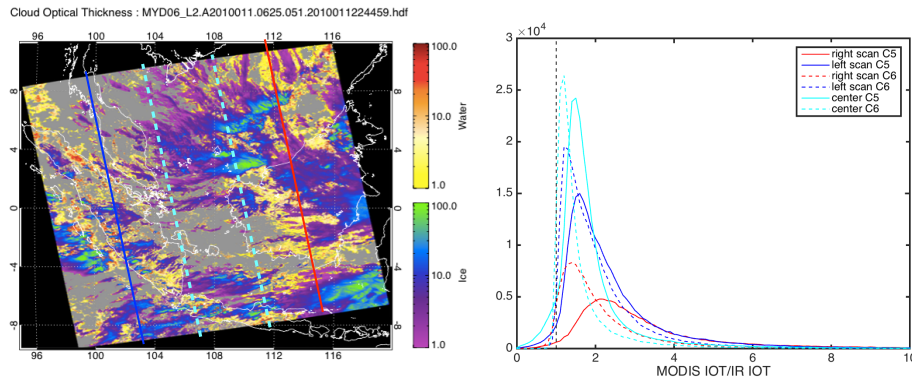


Figure 4. The MODIS IOT retrievals dependence on scan angle is investigated in the above panels. The image presents the MODIS C5 OT retrievals on 11 January 2010 at 06:25 UTC. The right panel presents a histogram of the ratio between the MODIS IOT for both C5 (solid line) and C6 (dashed line) and full swath IR retrieval for only those FOVs which were identified as ice by MODIS. The histograms are separated by view angle the approximate regions for each color marked by the associated color lines on the left image. Notice the significant scan dependent bias relative to the IR IOT for the MODIS C5 retrievals.

Title Page

Abstract

Introduction

Conclusions

References

Tables

Figures

◀

▶

◀

▶

Back

Close

Full Screen / Esc

Printer-friendly Version

Interactive Discussion



Resolving ice cloud optical thickness biases between CALIOP and MODIS

R. E. Holz et al.

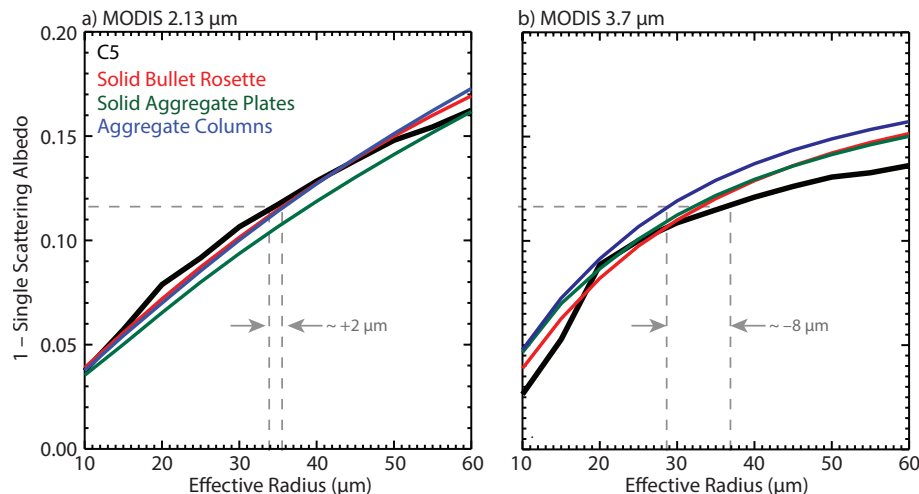


Figure 5. The relationship between effective radius and single scattering co-albedo in the MODIS **(a)** 2.13 and **(b)** 3.7 μm channels for different ice particle radiative models. See Fig. 6 for model details. Since effective radius retrievals for an optically thick cloud are a retrieval of co-albedo, the difference between the C5 and aggregated column model co-albedo implies a retrieved effective radius difference of +2 and $-8 \mu\text{m}$, respectively, for a C5 effective radius retrieval of about $35 \mu\text{m}$.

Title Page

Abstract

Introduction

Conclusions

References

Tables

Figures

◀

▶

◀

▶

Back

Close

Full Screen / Esc

Printer-friendly Version

Interactive Discussion



Resolving ice cloud optical thickness biases between CALIOP and MODIS

R. E. Holz et al.

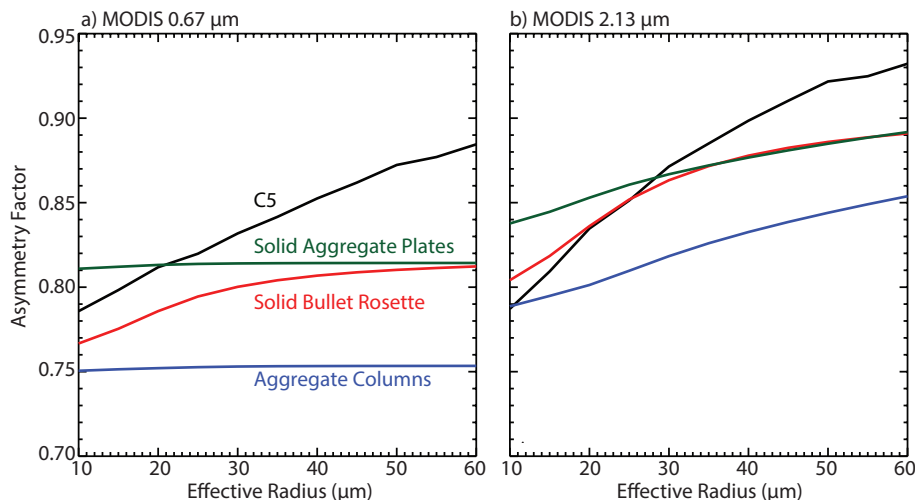


Figure 6. The relationship between effective radius and single scatter asymmetry parameter in the MODIS **(a)** 0.67 and **(b)** 2.13 μm channels for different ice particle radiative models. Notice the strong dependence of the MODIS C5 model asymmetry parameter on effective size. The other models consist of a single habit with severely roughened surfaces. The single habit calculations are made for a modified gamma size distribution and an effective variance of 0.10.

Title Page

Abstract

Introduction

Conclusions

References

Tables

Figures

◀

▶

◀

▶

Back

Close

Full Screen / Esc

Printer-friendly Version

Interactive Discussion



Resolving ice cloud optical thickness biases between CALIOP and MODIS

R. E. Holz et al.

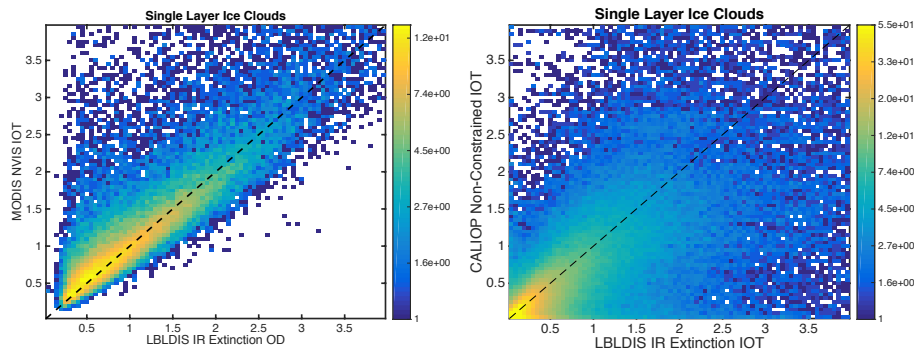


Figure 7. The joint histogram comparing the MODIS C6 IOT with the reference IOT retrieval **(a)**. Notice the significant improvement in the agreement resulting from the change to severely roughened aggregated columns. The CALIOP non-constrained IOT using a modified lidar ratio of 32 is compared to collocated IR MODIS retrieved IOT in the right panel **(b)**. Notice the significant improvement in the no-linear bias compared to Fig. 3b.

[Title Page](#)[Abstract](#)[Introduction](#)[Conclusions](#)[References](#)[Tables](#)[Figures](#)[◀](#)[▶](#)[◀](#)[▶](#)[Back](#)[Close](#)[Full Screen / Esc](#)[Printer-friendly Version](#)[Interactive Discussion](#)

Resolving ice cloud optical thickness biases between CALIOP and MODIS

R. E. Holz et al.

Title Page

Abstract

Introduction

Conclusions

References

Tables

Figures

◀

▶

◀

▶

Back

Close

Full Screen / Esc

Printer-friendly Version

Interactive Discussion

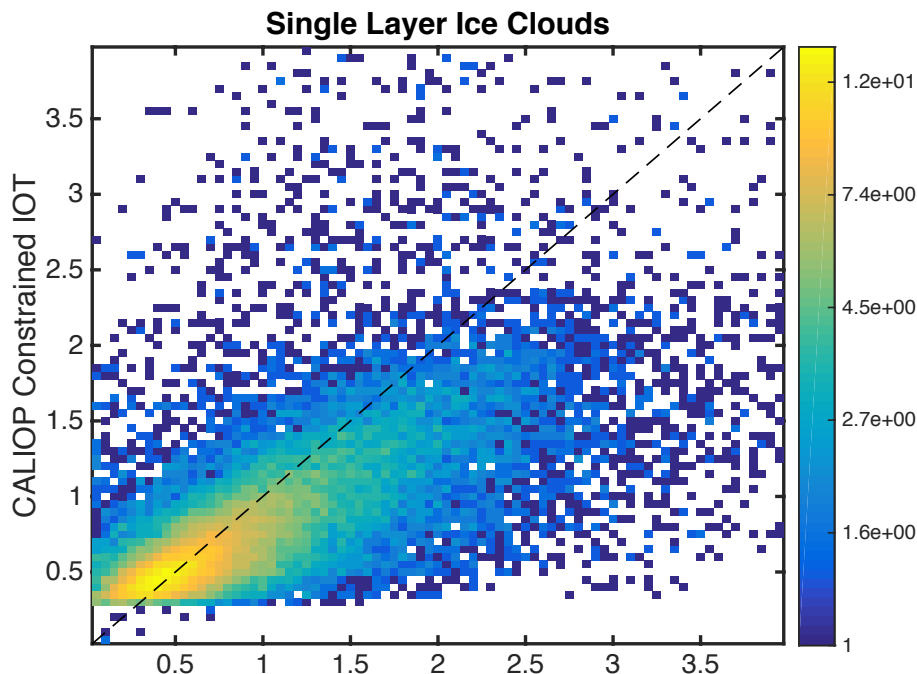


Figure 9. The CALIOP V3 constrained IOT retrieval for single layer clouds is compared to the LBLDIS reference IOT retrieval. Due to single to noise limitations the comparison is limited to nighttime only FOV.

Resolving ice cloud optical thickness biases between CALIOP and MODIS

R. E. Holz et al.

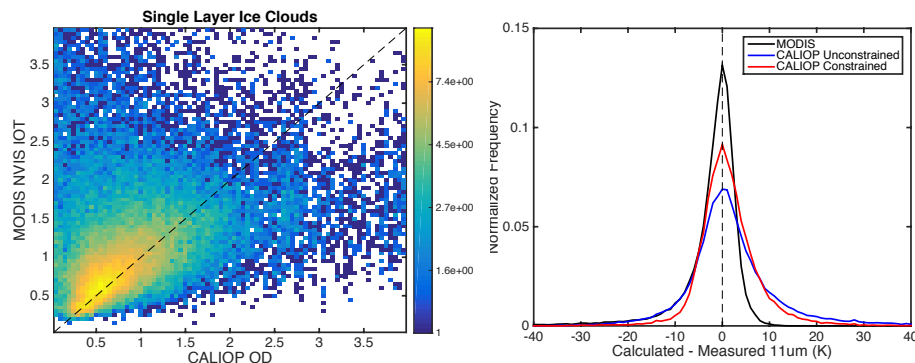


Figure 10. The CALIOP unconstrained IOT but processed using a modified lidar ratio of 32 is compared to the new single habit ice scattering LUT used in the updated MODIS C6 IOT retrievals in the left (a) panel. Notice the improved bias relative to the MODIS C5 and V3 CALIOP retrievals presented in Fig. 1. The radiative closure analysis using the updated retrievals is presented in the right (b) panel. The modifications have greatly improved agreement with the measured MODIS 11 μ m channel compared to MODIS C5 and the current V3 CALIOP retrievals presented in Fig. 2.